Supporting Information of

Comparison of phase states of $PM_{2.5}$ over megacities, Seoul and Beijing, and their implications on particle size distribution

Mijung Song[1,2], Rani Jeong[1], Daeun Kim[1], Yanting Qiu[3], Xiangxinyue Meng[3], Zhijun Wu[3], Andreas Zuend[4], Yoonkyeong Ha[5], Changhyuk Kim[5], Haeri Kim[1], Sanjit Gaikwad[1], Kyoung-Soon Jang[6], Jiyi Lee[7], Joonyoung Ahn[8]*

[1]Department of Environment and Energy, Jeonbuk National University, Jeollabuk-do Jeonju-si 54896, Republic of Korea; [2]Department of Earth and Environmental Sciences, Jeonbuk National University, Jeollabuk-do Jeonju-si 54896, Republic of Korea; [3]State Key Joint Laboratory of Environmental Simulation and Pollution Control, College of Environmental Sciences and Engineering, Peking University, Beijing 100871, China; [4]Department of Atmospheric and Oceanic Sciences, McGill University, Montréal, Quebec H3A 0B9, Canada; [5]School of Civil and Environmental Engineering, Pusan National University, Busan 46241, Republic of Korea; [6]Bio-Chemical Analysis Team, Korea Basic Science Institute, Cheongju 28119, Republic of Korea; [7]Department of Environmental Science & Engineering, Ewha Womans University, 52, Ewhayeodae-gil, Seodaemun-gu, Seoul 03760, Republic of Korea; [8]Department of Atmospheric

Environment Research, National Institute of Environmental Research, 215, Jinheung-ro, Eunpyeong-gu, Seoul 03367, Republic of Korea

*Corresponding Author: **Mijung Song** - Department of Environment and Energy, Jeonbuk National University, Jeollabuk-do Jeonju-si 54896; Department of Earth and Environmental Sciences Jeonbuk National University, Jeollabuk-do Jeonju-si 54896;

Email: Mijung.Song@jbnu.ac.kr

The supplemental materials include 26 pages

Section S1-S7

Figure S1-S8

References

Section S1. Site description

To investigate the phase state of $PM_{2.5}$ in megacities of northeast Asia, we selected two megacities of Seoul in South Korea and Beijing in China.[1] The sampling site in Seoul was the metropolitan area intensive air quality monitoring station (37.61 °N, 126.93 °E) operated by the National Institute of Environmental Research (NIER) in Bulgwang-dong, Eunpyeong-gu. As a megacity with a population of approximately 10 million in 2022, Seoul contains high amounts of traffic roads and residential complexes and can be considered a representative urban site in South Korea.[2] Beijing is one of the biggest megacities in northeast Asia with a population of almost 21 million in 2022.[3] The sampling site in Beijing was located on the fourth floor building in the Changping campus of Peking University (40.25 °N, 116.19 °E), ~ 40 km away from the center of the city surrounded by traffic roads that cause heavy emission of particulate matter. Field campaigns were conducted simultaneously in the two megacities from December 15, 2020 to January 14, 2021.

Section S2. Preparation of droplets of $PM_{2.5}$

The water-soluble species in the $PM_{2.5}$ filters were extracted in purified water (18.2 MΩ·cm, Millipore, USA). Previous studies have been reported that water-soluble species are most abundant in $PM_{2.5}$, accounting for > ~70%.[4-6] Observation of particle morphology using this extraction method has been reported previously.[7,8] The $PM_{2.5}$ extracts were nebulized on a hydrophobic substrate (Hampton Research, Canada) using a nebulizer (MEINHARD®, Perkin Elmer, USA) and the substrate was then mounted in a flow-cell that can control relative humidity (RH)[9] for morphology observations (see Section 2.2) and poke-and-flow experiments (see Section 2.3).

Section S3. Chemical compositions and meteorological parameters

The chemical compositions and meteorological parameters in the two cities during the measurement periods have been reported in Kim et al.[10] and Qiu et al.[11] In brief, hourly $PM_{2.5}$ mass concentrations were measured simultaneously using a β-ray particulate monitor (model 5014i, Thermo Scientific Inc.) in Seoul and a tapered element oscillating microbalance (TH-2000Z1, Wuhan Tianhong Inc.) in Beijing.

For the chemical compositions, $PM_{2.5}$ in Seoul and $PM_{1.0}$ in Beijing were analyzed. In Seoul, hourly concentrations of inorganic substances (SO_4^{2-}, NO_3^-, Cl^-, Na^+, NH_4^+, K^+, Mg^{2+}, and Ca^{2+}) (Ambient Ion Monitor, URG Corporation, USA), organic carbon (OC), and elemental carbon (EC) (SECOC Analyzer, Sunset Laboratory Inc., USA) of $PM_{2.5}$ were measured. To compare with the organic aerosol (OA) concentration in Beijing, the OC concentration in Seoul was converted to OA concentration based on the consideration of 1.8 for OA/OC ratio in Seoul.[10,12] In Beijing, simultaneously, hourly concentrations of the inorganic substances (SO_4^{2-}, NO_3^-, Cl^-, and NH_4^+) and OA and EC of $PM_{1.0}$ were measured (Quadrupole Aerosol Chemical Speciation Monitor[13], equipped with a standard vaporizer, Aerodyne Research, USA).

Meteorological parameters, such as temperature, RH, wind speed, wind direction, and precipitation were measured by the NIER (Metone Inc.) in Seoul and an automatic meteorological station (Metone Inc.) in Beijing.[10,11] In this study, all data used were based on the interval of the filter sampling (10:00 to 09:00 a.m. of the following day in local time). Table 1 summarizes the daily average concentrations of meteorological parameters and chemical compositions in both cities.

Section S4. Analysis of elemental oxygen-to-carbon ratios

The elemental oxygen-to-carbon ratio (O:C) of water-soluble organic carbon (WSOC) in the $PM_{2.5}$ filter sample was measured using an ultrahigh-resolution Fourier-transform ion cyclotron

resonance mass spectrometer (FT-ICR MS).[14] Briefly, the WSOC extracts of the filter samples were analyzed using a 15 Tesla FT-ICR MS (solariX XR™ system, Bruker Daltonics, Billerica, MA, USA) via negative electrospray ionization to conduct highly accurate mass measurement of the $PM_{2.5}$-derived WSOC samples. After the acquisition of FT-ICR MS spectra, the assignment of elemental compositions of WSOC was performed from the FT-ICR MS datasets using DataAnalysis (ver. 4.2, Bruker Daltonics) and Composer (Sierra Analytics, Modesto, CA) software. All possible molecular formulas were calculated by using atomic combinations of $C_{1\text{-}200}H_{1\text{-}400}O_{0\text{-}60}N_{0\text{-}4}S_{0\text{-}2}$ from the observed masses of singly charged molecular ions in the range of 150-1000 *m/z*. Invalid assignments to the constraints (i.e., nitrogen rule, $H \leq 2C + 2 + N$, atomic $O/C \leq 1$, $N/C \leq 1$, $H/C > 0.3$, and $DBE > 0$) were excluded from the list of assigned molecular formulas. We also excluded the molecular formulas that had a mass error of 0.3 ppm or more and were obtained from the blank filter extract. The daily O:C ratios were finally estimated by averaging the individual O:C ratios of the molecular formulas assigned from WSOC in the filters. The detailed procedure and method can be found in previous studies.[7,15]

Section S5. Rebound fraction

The result of phase states of $PM_{2.5}$ from Beijing filter samples obtained from the optical microscopy combined with the poke-and-flow technique was compared with a different technique of rebound fraction using a three-arm impactor. A detailed description of the three-arm impactor was given by Bateman et al.[16] and Liu et al.[17]. In this study, the same method and procedure were used as described in Liu et al.[17]. In brief, a three-arm impactor, combined with a condensation particle counter (CPC, TSI model 3772), was used to obtain hourly average rebound fractions of ~ 300 nm in Beijing during the measurement periods. The impactor measures the probability of rebound when the PMs collide with a hard surface as follows. If the rebound energy is less than

the adhesion energy, the PMs stick to the surface and are considered to be liquid (rebound fraction < 0.2). Conversely, if the PMs rebound from the surface, they are considered to be (semi)solid (rebound fraction > 0.2).

Figure S6 compares the particle phase states in Beijing at the same time/dates using the two different techniques of microscopic observation combined with the poke-and-flow technique for the Beijing $PM_{2.5}$ filter samples (Figure S6A, see Section 3.1) and the daily averaged rebound fractions of submicron-particles monitored in Beijing (Figure S6B). The phase states on each date in Beijing are in good agreement from the two different methods even though the particle size ranges were different ($PM_{2.5}$ vs. ~300 nm).

Section S6. Calculation of aerosol liquid water content

To estimate the aerosol liquid water content (ALWC) of $PM_{2.5}$ in Seoul and Beijing, we used the thermodynamic equilibrium model ISORROPIA-II. This model is an extensively used and is computationally efficient based on the Cl^--NO_3^-–SO_4^{2-}–Ca^{2+}–K^+–Mg^{2+}–NH_4^+–Na^+–H_2O aerosol system.[18,19] For the input data, the hourly concentrations of inorganic species (SO_4^{2-}, NO_3^-, Cl^-, Na^+, K^+, NH_4^+, Ca^{2+}, and Mg^{2+}) of $PM_{2.5}$ in Seoul and of $PM_{1.0}$ in Beijing, and meteorological parameters (temperature and RH) in each site were used. In this study, ISORROPIA-II was operated in the "metastable" mode, assuming that particles are composed of an aqueous sub- or supersaturated solution that prevents the formation of solid precipitates. The ALWC was estimated based on the "reverse" mode calculation, in which the known input quantities were the concentrations of the inorganic species in the aerosol phase, temperature, and RH. The ALWC depends on ambient particle composition and RH; it tends to increase with increasing RH. The ALWC associated with higher fractions of inorganics was greater than that associated with lower fractions of inorganics at a constant RH; as expected from hygroscopicity and gas–particle

partitioning theory.[20] Thus, the increase in the ALWC for a given RH was larger for particles with greater inorganic mass fractions. Some studies have shown that the ALWC might be underestimated because the hygroscopicity of organic compounds is not considered.[18,20] However, studies have also shown that the correlation coefficient between the observed hygroscopic diameter growth factors and the simulated ALWC by ISORROPIA-II agreed well with values of ~0.76[21] and ~0.89.[20]

Section S7. Particle number and volume size distributions for geometric number and volume diameters

The particle number size distribution (PNSD) of the atmospheric $PM_{2.5}$ was measured using a regular scanning mobility particle sizer (RSMPS, model 3938, TSI Inc.) every 5 min in Seoul and Beijing (11 – 460 and 12 – 590 nm, respectively). Then, the hourly averaged PNSD for the two cities was obtained from the measured PNSD with a 5-min time resolution, as shown in Figure S7. The particle volume size distribution (PVSD) was obtained from the PNSD by assuming that particles were spherical. For comparing the characteristics of the particle growth according to the particle viscosity between the two cities, the geometric number diameter (GMD_N) was calculated from the hourly averaged PNSD for each city. The GMD_N was calculated from 20 to 470 nm of each hourly averaged PNSD to avoid the low counting efficiency of the RSMPS below 20 nm, as well as to be able to compare the same particle size range between Seoul and Beijing. The GMD_N and GMD_V of $PM_{2.5}$ were calculated following the method.[11,22]

$$\mathrm{GMD_N} = \sqrt[N_{tot}]{\prod_{k=1}^{k=n} D_{p_k}^{dN_k}} \quad (1)$$

$$\mathrm{GMD_V} = \sqrt[V_{tot}]{\prod_{k=1}^{k=n} D_{p_k}^{dV_k}} \quad (2)$$

, where dN_k and dV_k are the number and volume concentrations of particles in the size bin (particles/cm^3 and nm^3/cm^3, respectively) which has midpoint $D_p = D_{pk}$, n is number of size bin. N_{tot} and V_{tot} are the total number and volume concentrations of particles of the whole PNSD and PVSD, which were determined as,

$$N_{tot} = \sum_{k=1}^{k=n} \frac{dN_k}{d\log D_{p_k}} d\log D_{p_k} \quad (3)$$

$$V_{tot} = \sum_{k=1}^{k=n} \frac{dV_k}{d\log D_{p_k}} d\log D_{p_k} \quad (4)$$

After obtaining the time-dependent GMD_N and GMD_V for each PNSD and PVSD, the daily averaged GMD_N and GMD_V distribution were also calculated for each city. Therefore, GMD_N generally followed the $PM_{2.5}$ mass concentration as discussed by Ha et al.[22] GMD_N is generally followed the change of $PM_{2.5}$ mass concentrations, which showed the growth of particles. GMD_V gives information of the particle size, which dominantly contributed to the $PM_{2.5}$ mass concentration at the moment. GMD_V was generally in the accumulation mode and larger than GMD_N during the campaign.

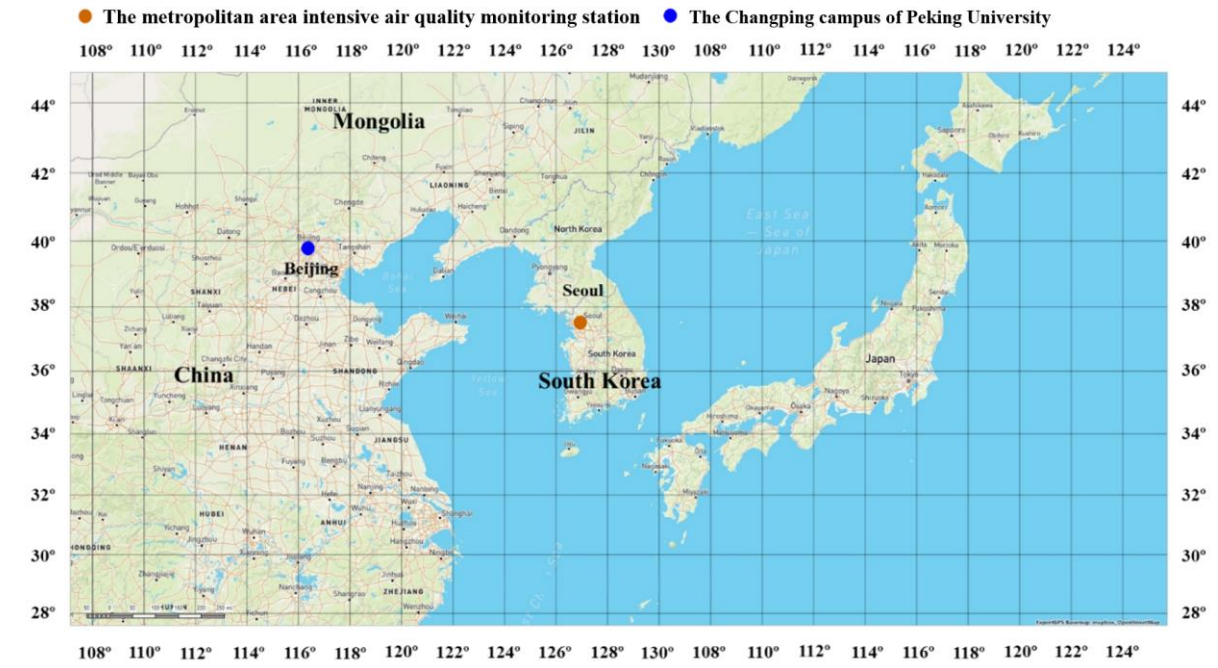

Figure S1. Location of the measurement sites in megacities, Seoul and Beijing, of northeast Asia.

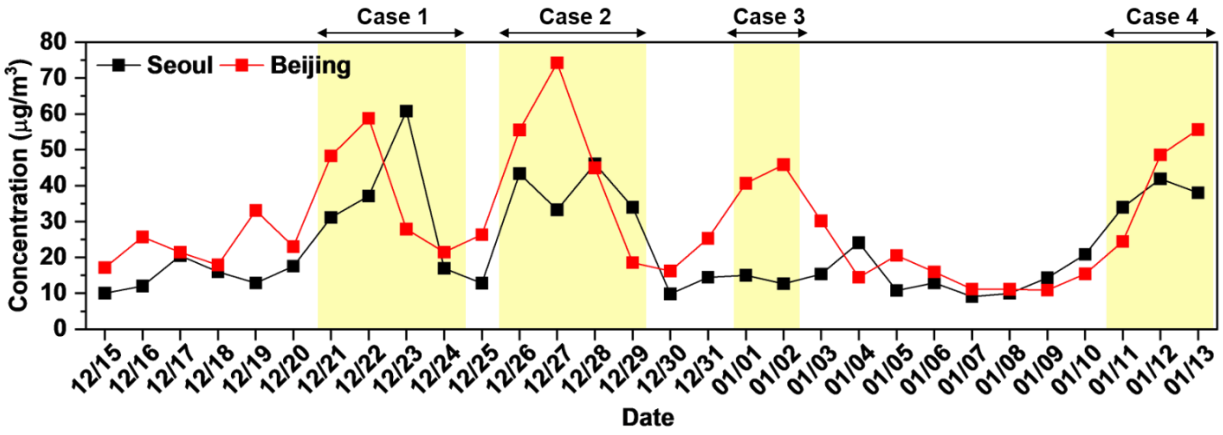

Figure S2. Variations of daily mean mass concentration of $PM_{2.5}$ in Seoul and Beijing over the entire period. Yellow shaded regions indicate "Cases 1 – 4" for $PM_{2.5}$ pollution episodes.

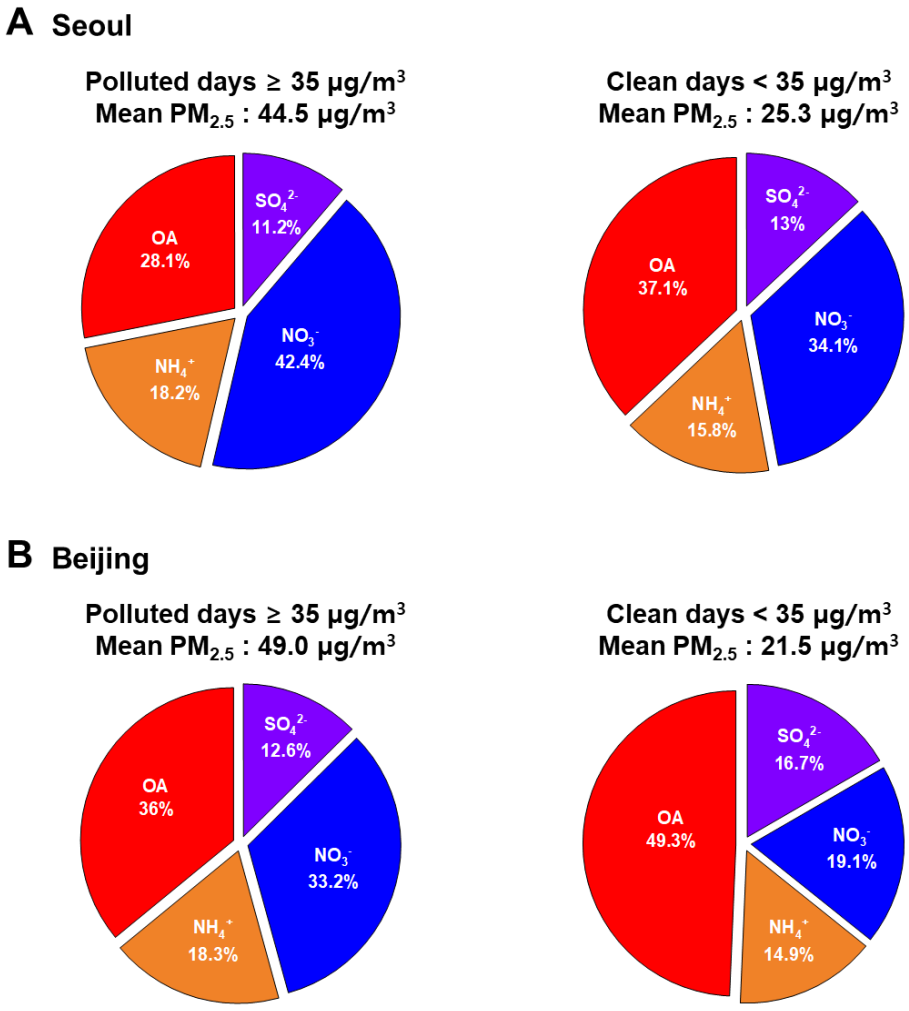

Figure S3. Mass concentration of $PM_{2.5}$ during polluted and clean days for Cases 1 - 4 in (A) Seoul and (B) Beijing. Mass fractions of the major chemical species of $PM_{2.5}$ in Seoul and of $PM_{1.0}$ in Beijing on polluted and clean days are also shown.

A

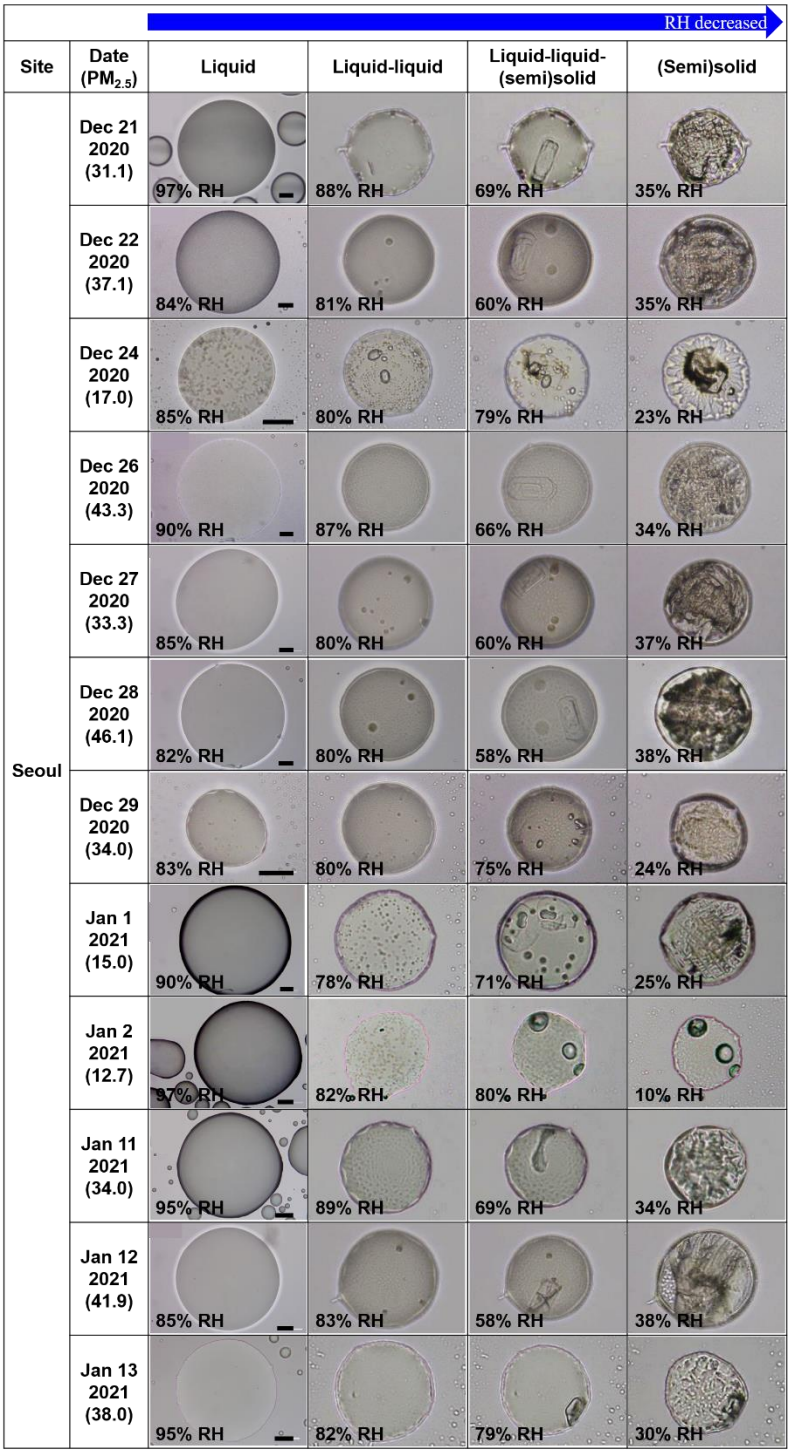
RH decreased
Site
Date (PM2.5)
Liquid
Liquid-liquid
Liquid-liquid-(semi)solid
(Semi)solid
Seoul
Dec 21 2020 (31.1)
97% RH
88% RH
69% RH
35% RH
Dec 22 2020 (37.1)
84% RH
81% RH
60% RH
35% RH
Dec 24 2020 (17.0)
85% RH
80% RH
79% RH
23% RH
Dec 26 2020 (43.3)
90% RH
87% RH
66% RH
34% RH
Dec 27 2020 (33.3)
85% RH
80% RH
60% RH
37% RH
Dec 28 2020 (46.1)
82% RH
80% RH
58% RH
38% RH
Dec 29 2020 (34.0)
83% RH
80% RH
75% RH
24% RH
Jan 1 2021 (15.0)
90% RH
78% RH
71% RH
25% RH
Jan 2 2021 (12.7)
97% RH
82% RH
80% RH
10% RH
Jan 11 2021 (34.0)
95% RH
89% RH
69% RH
34% RH
Jan 12 2021 (41.9)
85% RH
83% RH
58% RH
38% RH
Jan 13 2021 (38.0)
95% RH
82% RH
79% RH
30% RH

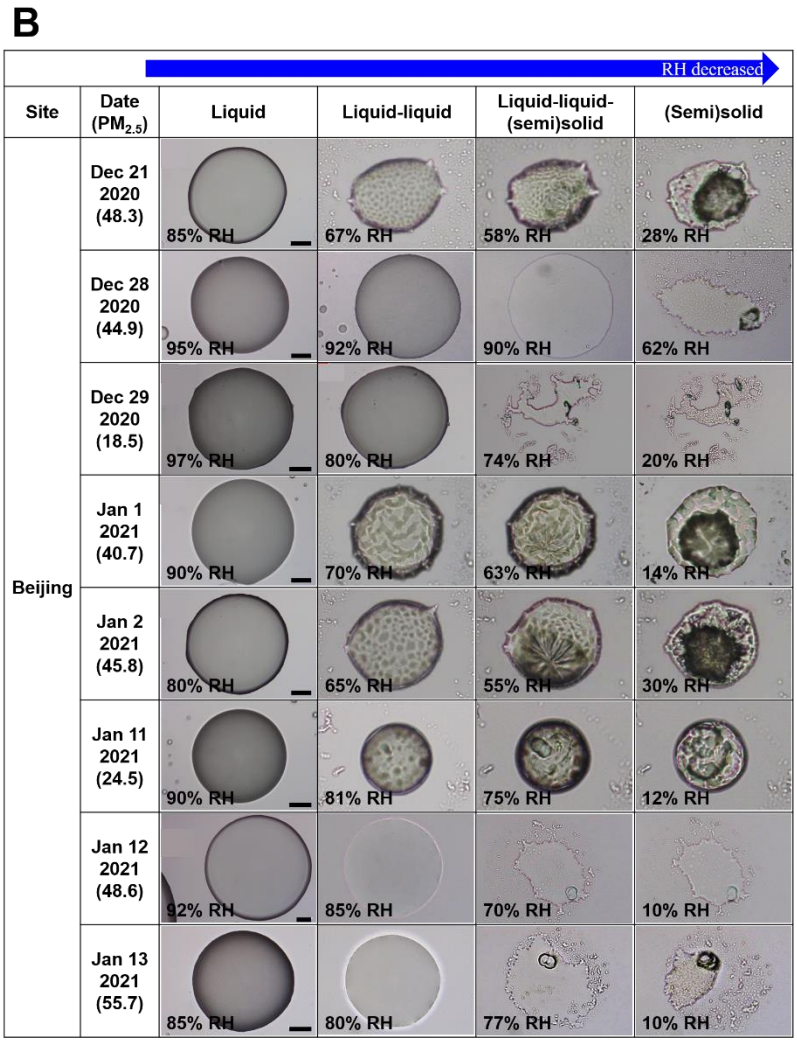

Figure S4. Optical images of morphology changes of $PM_{2.5}$ in (A) Seoul and (B) Beijing samples on each date with decreasing relative humidity (RH) at 290 K. The black scale bar indicates 10 μm.

A

Site	Date $PM_{2.5}$	RH	Pre-poking	Poking	After 0 second	After 1 hour	After 3 hour
Seoul	Dec 21 2020 (31.1)	30	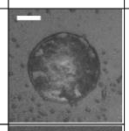		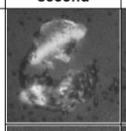	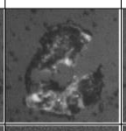	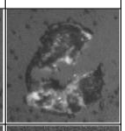
	Dec 22 2020 (37.1)	30	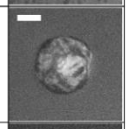		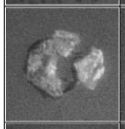	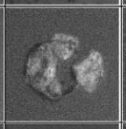	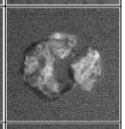
	Dec 24 2020 (17.0)	30	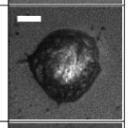		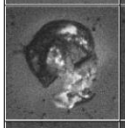	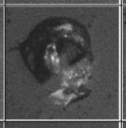	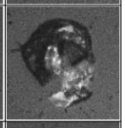
	Dec 26 2020 (43.3)	30	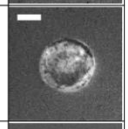		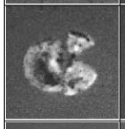	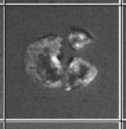	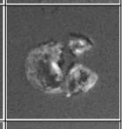
	Dec 27 2020 (33.3)	30	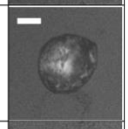		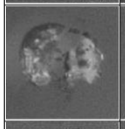	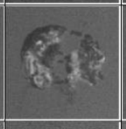	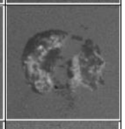
	Dec 28 2020 (46.1)	30	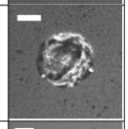		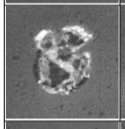	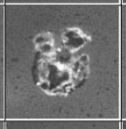	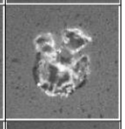
	Dec 29 2020 (34.3)	20	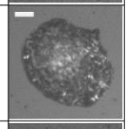		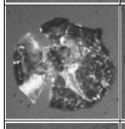	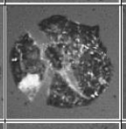	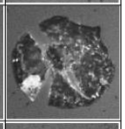
	Jan 1 2021 (15.0)	20	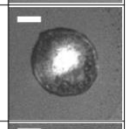		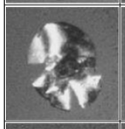	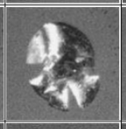	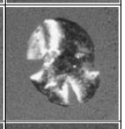
	Jan 2 2021 (12.7)	10	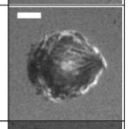		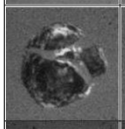	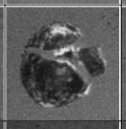	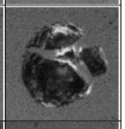
	Jan 11 2021 (34.0)	30	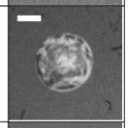		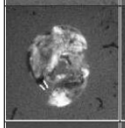	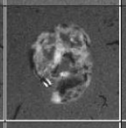	
	Jan 12 2021 (41.9)	30					
	Jan 13 2021 (38.0)	20					

B

Site	Date ($PM_{2.5}$)	RH	Pre-poking	Poking	After 0 second	After 1 hour	After 3 hour
Beijing	Dec 21 2020 (48.3)	20	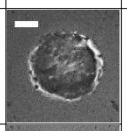		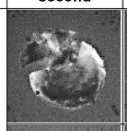	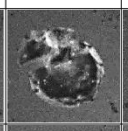	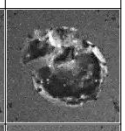
	Dec 28 2020 (44.9)	10	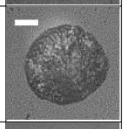		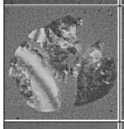	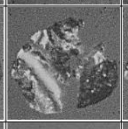	
	Dec 29 2020 (18.5)	20	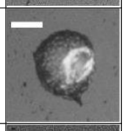		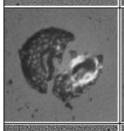	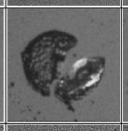	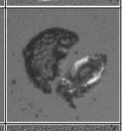
	Jan 1 2021 (40.7)	20	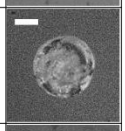		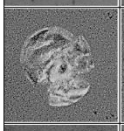	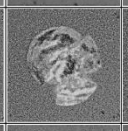	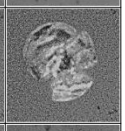
	Jan 2 2021 (45.8)	20	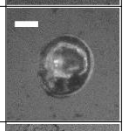		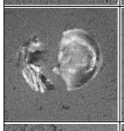	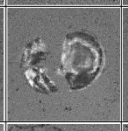	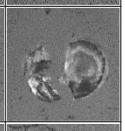
	Jan 11 2021 (24.5)	10	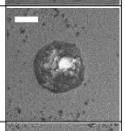		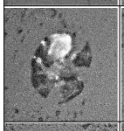	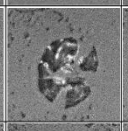	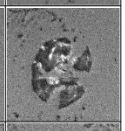
	Jan 12 2021 (48.6)	10	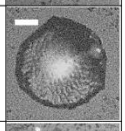		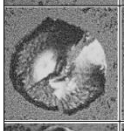		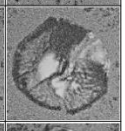
	Jan 13 2021 (55.7)	10	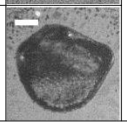		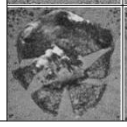		

Figure S5. Optical images during the poke-and-flow experiments at 293 K. Images are shown on pre-poking, poking and post-poking of $PM_{2.5}$ in (A) Seoul and (B) Beijing samples. The white scale bar indicates 10 μm.

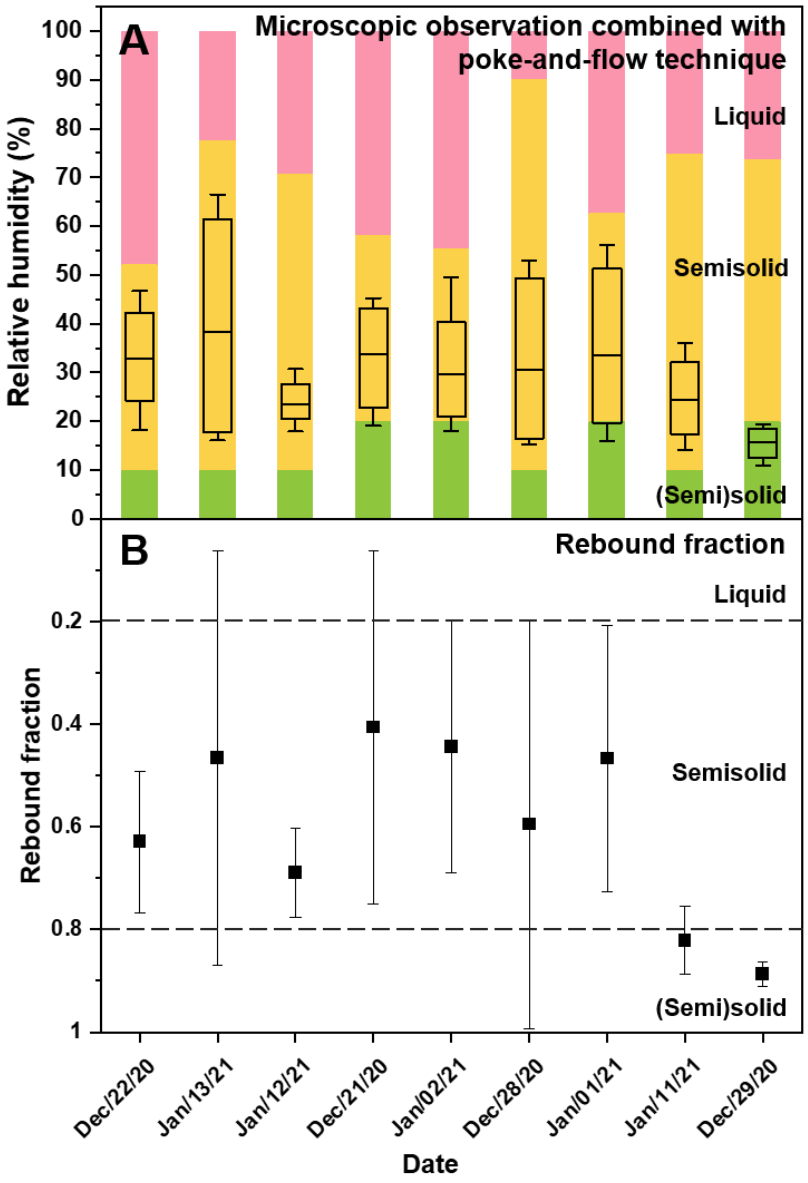

Figure S6. A comparison of daily averaged particle phase states (A) in Beijing $PM_{2.5}$ filter samples using optical microscopy combined with the poke-and-flow technique (same figure shown in Figure 2D), and (B) in Beijing using a rebound fraction from a field measurement. Dates are shown in order from high to low $PM_{2.5}$ concentrations. In figure (A), ambient relative humidity is in the box plot with daily mean, 25th, and 75th percentiles, minimum and maximum. In figure (B), solid squares indicate daily mean rebound fraction and the error bars are the standard deviation.

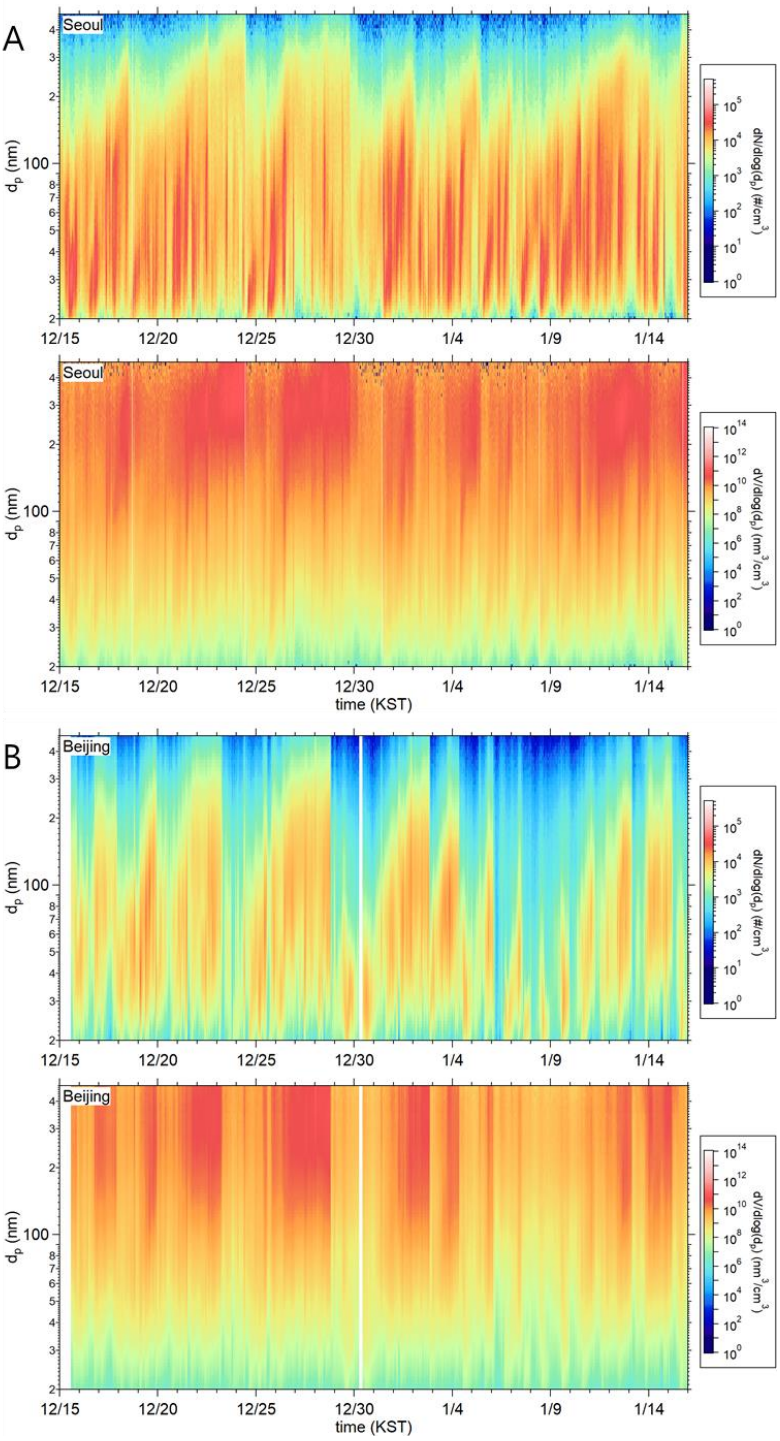

Figure S7. Particle number and volume size distributions ($dN/dlogD_p$ and $DV/dlogD_p$, respectively) of $PM_{2.5}$ measured in (A) Seoul and (B) Beijing, 20 – 470 nm. Particle growth from

nucleation mode (D_p < 23 nm) to accumulation mode (100 nm < D_p < 1 μm) was observed in the particle number size distribution in each city.

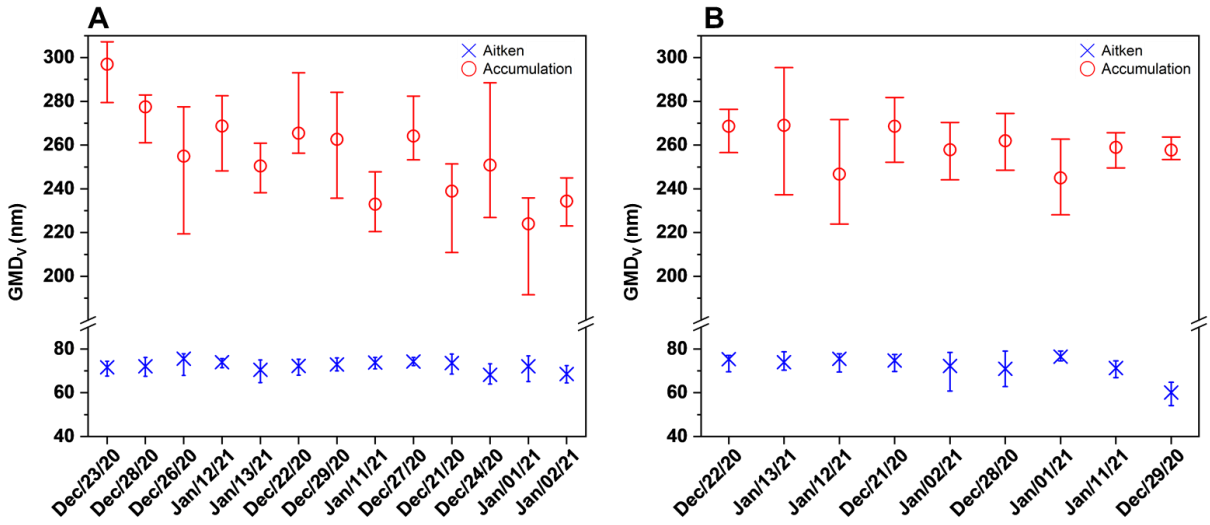

Figure S8. Particle geometric volume mean diameters (GMD_V) of Aitken (20 – 100 nm) and accumulation (100 – 470 nm) mode of each hourly averaged particle size distribution for (A) Seoul and (B) Beijing, respectively. Dates are arranged from high to low daily mean $PM_{2.5}$ concentrations as shown in Figure 2.

References:

(1) The World's cities in 2018 : data booklet. https://digitallibrary.un.org/record/3799524 (accessed 2018-07-31).

(2) Korean Statistical Information Service (KOSIS). https://kosis.kr (accessed 2022-06-13).

(3) Macrotrends Beijing, China Metro Area Population 1950-2022. https://www.macrotrends.net/cities/20464/beijing/population (accessed 2022-06-13).

(4) Liu, Y.; Li, H.; Cui, S.; Nie, D.; Chen, Y.; Ge, X. Chemical Characteristics and Sources of Water-Soluble Organic Nitrogen Species in PM2. 5 in Nanjing, China. *Atmosphere.* **2021,** *12*, 574.

(5) Huang, H.; Ho, K. F.; Lee, S.; Tsang, P.; Ho, S. S. H.; Zou, C.; Zou, S.; Cao, J.; Xu, H. Characteristics of carbonaceous aerosol in PM2. 5: Pearl Delta River region, China. *Atmos. Res.* **2012,** *104*, 227-236.

(6) Sudheer, A.; Aslam, M.; Upadhyay, M.; Rengarajan, R.; Bhushan, R.; Rathore, J.; Singh, S.; Kumar, S. Carbonaceous aerosol over semi-arid region of western India: Heterogeneity in sources and characteristics. *Atmos. Res.* **2016,** *178*, 268-278.

(7) Gaikwad, S.; Jeong, R.; Kim, D.; Lee, K.; Jang, K.-S.; Kim, C.; Song, M. Microscopic observation of a liquid-liquid-(semi) solid phase in polluted PM2.5. *Front.* **2022**, 1126.

(8) You, Y.; Renbaum-Wolff, L.; Carreras-Sospedra, M.; Hanna, S. J.; Hiranuma, N.; Kamal, S.; Smith, M. L.; Zhang, X.; Weber, R. J.; Shilling, J. E.; Dabdub, D.; Martin, S. T.; Bertram, A. K. Images reveal that atmospheric particles can undergo liquid-liquid phase separations. *Proc. Natl. Acad. Sci.* **2012,** *109*, 13188-13193.

(9) Song, Y.-C.; Bé, A. G.; Martin, S. T.; Geiger, F. M.; Bertram, A. K.; Thomson, R. J.; Song, M. Liquid–liquid phase separation and morphologies in organic particles consisting of α-pinene and β-caryophyllene ozonolysis products and mixtures with commercially available organic compounds. *Atmos. Chem. Phys.* **2020,** *20*, 11263-11273.

(10) Kim, N. K.; Kim, Y. P.; Ghim, Y. S.; Song, M.; Kim, C. H.; Jang, K. S.; Lee, K. Y.; Shin, H. J.; Jung, J. S.; Wu, Z.; Matsuki, A.; Tang, N.; Sadanaga, Y.; Shungo, K.; Natsagdorj, A.; Tseren-Ochir, S.-E.; Baldorj, B.; Song, C. K.; Lee, J. Y. Spatial distribution of PM2.5

chemical components during winter at five sites in Northeast Asia: High temporal resolution measurement study. *Atmos. Environ.* **2022**, *290*, 119359.

(11) Qiu, Y.; Wu, Z.; Man, R.; Zong, T.; Liu, Y.; Meng, X.; Chen, j.; Chen, S.; Yang, S.; Yuan, B.; Song, M.; Kim, C. H.; Ahn, J.; Zeng, L.; Lee, J. Y.; Hu, M. Secondary Aerosol Formation Drives the Particulate Matter Pollution in the Megacities (Beijing and Seoul) over East Asia. *Atmos. Environ.* **2022**, (in review).

(12) Kim, H.; Zhang, Q.; Heo, J. Influence of intense secondary aerosol formation and long-range transport on aerosol chemistry and properties in the Seoul Metropolitan Area during spring time: results from KORUS-AQ. *Atmos. Chem. Phys.* **2018,** *18*, 7149-7168.

(13) Ng, N. L.; Herndon, S. C.; Trimborn, A.; Canagaratna, M. R.; Croteau, P.; Onasch, T. B.; Sueper, D.; Worsnop, D. R.; Zhang, Q.; Sun, Y. An Aerosol Chemical Speciation Monitor (ACSM) for routine monitoring of the composition and mass concentrations of ambient aerosol. *Aerosol Sci. Tech.* **2011,** *45*, 780-794.

(14) Jang, K.-S.; Choi, M.; Park, M.; Park, M. H.; Kim, Y. H.; Seo, J.; Wang, Y.; Hu, M.; Bae, M.-S.; Park, K. Assessment of PM2.5-bound nitrogen-containing organic compounds (NOCs) during winter at urban sites in China and Korea. *Environ. Pollut.* **2020,** *265*, 114870.

(15) Choi, J. H.; Ryu, J.; Jeon, S.; Seo, J.; Yang, Y.-H.; Pack, S. P.; Choung, S.; Jang, K.-S. In-depth compositional analysis of water-soluble and-insoluble organic substances in fine (PM2. 5) airborne particles using ultra-high-resolution 15T FT-ICR MS and GC× GC-TOFMS. *Environ. Pollu.* **2017,** *225*, 329-337.

(16) Bateman, A. P.; Belassein, H.; Martin, S. T. Impactor apparatus for the study of particle rebound: Relative humidity and capillary forces. *Aerosol. Sci. Technol.* **2014,** *48*, 42-52.

(17) Liu, Y.; Wu, Z.; Wang, Y.; Xiao, Y.; Gu, F.; Zheng, J.; Tan, T.; Shang, D.; Wu, Y.; Zeng, L. Submicrometer particles are in the liquid state during heavy haze episodes in the urban atmosphere of Beijing, China. *Environ. Sci. Technol. Lett.* **2017,** *4*, 427-432.

(18) Fountoukis, C.; Nenes, A. ISORROPIA II: a computationally efficient thermodynamic equilibrium model for K+;Ca2+;Mg+;NH+;Na+;SO42-;NO3-;Cl-;H2O aerosols. *Atmos. Chem. Phys.* **2007,** *7*, 4639-4659.

(19) Fountoukis, C.; Nenes, A.; Sullivan, A.; Weber, R.; Van Reken, T.; Fischer, M.; Matías, E.; Moya, M.; Farmer, D.; Cohen, R. C. Thermodynamic characterization of Mexico City aerosol during MILAGRO 2006. *Atmos. Chem. Phys.* **2009,** *9*, 2141-2156.

(20) Jin, X.; Wang, Y.; Li, Z.; Zhang, F.; Xu, W.; Sun, Y.; Fan, X.; Chen, G.; Wu, H.; Ren, J. Significant contribution of organics to aerosol liquid water content in winter in Beijing, China. *Atmos. Chem. Phys.* **2020,** *20*, 901-914.

(21) Shen, X.; Sun, J.; Zhang, X.; Zhang, Y.; Zhong, J.; Wang, X.; Wang, Y.; Xia, C. Variations in submicron aerosol liquid water content and the contribution of chemical components during heavy aerosol pollution episodes in winter in Beijing. *Sci. Total Environ.* **2019,** *693*, 133521.

(22) Ha, Y.; Kim, J.; Lee, S.; Cho, K.; Shin, J.; Kang, G.; Song, M.; Lee, J.; Jang, K. S.; Lee, K.; Ahn, J.; Wu, Z.; Matsuki, A.; Tang, N.; Sadanaga, Y.; Natsagdorj, A.; Kim, C. Spatiotemporal Differences on the Real-time Physicochemical Characteristics of PM2.5 Particles in Four Northeast Asian Countries During Winter and Summer 2020-2021. *Atmos. Res.* **2022**, (in review).